In "Ord. and Partial Diff. eqns"
: Lect. Notes in Maths, 1151, pp 252-269, Springer (198

A MECHANICAL MODEL FOR BIOLOGICAL PATTERN FORMATION: A NONLINEAR BIFURCATION ANALYSIS

P.K. Maini, J.D. Murray and G.F. Oster

Abstract

We present a mechanical model for cell aggregation in embryonic development. The model is based on the large traction forces exerted by fibroblast cells which deform the extracellular matrix (ECM) on which they move. It is shown that the subsequent changes in the cell environment can combine to produce pattern. A linear analysis is carried out for this model. This reveals a wide spectrum of different types of dispersion relations. A non-linear bifurcation analysis is presented for a simple version of the field equations: a non-standard element is required. Biological applications are briefly discussed.

1. INTRODUCTION

A central question in developmental biology is the process by which geometrical patterns emerge during embryogenesis. Several models have been proposed to describe the mechanisms of development of biological form (morphogenesis). Turing (1952) showed how a system of reacting and diffusing chemicals (morphogens) could produce pattern due to instability of a homogeneous equilibrium state. Such reaction-diffusion models have been widely studied since (e.g. Gierer and Meinhardt (1972), Thomas (1975), Murray (1977, 1981), Meinhardt (1982)).

A somewhat simpler scheme is the gradient model (Wolpert (1969)), which supposes the existence of a group of morphogen secreting cells (e.g. Saunders and Gasseling (1968)). The morphogen diffuses away from the source setting up a stationary gradient. Cells differentiate when the concentration of the morphogen reaches a certain threshold value (Smith and Wolpert (1981), Wolpert and Hornbruch (1981), Smith et al (1978), Tickle (1981)).

The central principle underlying these models is the setting up of a chemical pre-pattern to which the cells respond. However, such models have certain problems: (i) except in rather special cases, the morphogens remain, as yet, unidentified; (ii) the mechanism by which cells respond to the concentration of morphogen is vague and, in general, must be exquisitely sensitive.

In this paper we present a mechanism for spatially patterning populations of mesenchymal cells which is based on the following well documented mechanical properties (Harris et al (1981)): 1) Cells spread and migrate within a substratum consisting of a fibrous extracellular matrix (ECM). 2) They generate large contractile forces which deform the ECM.

Section 2 contains a brief resume of the model equations; the reader is referred to the paper by Oster, Murray and Harris (1983) (and references therein) for full details. Section 3 contains a linear analysis of the model. This gives rise to an abundance of dispersion relations, suggesting a richness in the pattern forming abilities of the model. In Section 4 a non-linear bifurcation analysis is presented on a simplified version of the model. This gives certain predictions for the amplitude of the heterogeneous cell density. The biological applications to long-standing problems of feather germ formation and wound healing are discussed at the end of the paper.

2. CELL TRACTION MODEL MECHANISM

The model is based on the three field variables

$n(\underline{x},t)$ = density of mesenchymal cells at position $\underline{x}$ and time t

$\rho(\underline{x},t)$ = density of ECM at position $\underline{x}$ and time t

$\underline{u}(\underline{x},t)$ = displacement at time t of a material point in the matrix which was initially at $\underline{x}$.

The equation for cell movement is

$$\frac{\partial n}{\partial t} = \nabla.\ (D_1(\underline{\underline{\varepsilon}})\nabla n - D_2(\underline{\underline{\varepsilon}})\nabla^3 n - \alpha[n\nabla(\rho+\alpha'\nabla^2\rho)] - n\frac{\partial \underline{\underline{u}}}{\partial t}) + rn(N-n) \qquad (1)$$

random dispersal haptotaxis convection mitosis

where $\underline{\underline{\varepsilon}} = 1/2[\nabla\underline{u} + \nabla\underline{u}^T]$ is the linear strain tensor. We motivate each of these terms in turn.

Random dispersal. We model this with a Fickian flux: $\underline{J} = -D_1(\underline{\underline{\varepsilon}})\nabla n$ where $D_1(\underline{\underline{\varepsilon}})$ is a strain dependent (i.e. matrix directed) diffusion coefficient. However, at large cell densities, Fick's Law is inadequate because it does not take into account non-local effects. These effects are important here because mesenchymal cells can detect non-local concentrations via long cell protuberances (filopodia). Thus cell movement also depends on the average cell concentration in the immediate surrounding. This average may be modelled by including a higher order term, $D_2(\underline{\underline{\varepsilon}})\nabla^3 n$, in the flux expression, where $D_2(\underline{\underline{\varepsilon}})$ is the long range diffusion coefficient: for simplicity we take $D_1(\underline{\underline{\varepsilon}})$ and $D_2(\underline{\underline{\varepsilon}})$ to be constant in this paper. Thus the random dispersal flux is modelled as

$$\underline{J}_{\text{random}} = -D_1\nabla n + D_2\nabla^3 n.$$

Note that the sign accompanying D_2 is plus. This implies that D_2, like D_1, is dispersive.

Haptotaxis. Cells actively move by attaching their filopodia to certain specialized adhesive sites on the extracellular matrix. They tend to move up a gradient in adhesive sites (haptotaxis) because the filopodia have a better grip where there are more adhesive sites and will thus drag the cell up the gradient (Harris (1973)). Assuming the adhesive sites are uniformly situated throughout the matrix, we have

$$\underline{J}_{\text{haptotaxis}} = \alpha n\nabla(\rho + \alpha'\nabla^2\rho)$$

where the $\nabla^2\rho(\underline{x},t)$ term takes into account long range interactions (c.f. long range diffusion).

Convection. Cells may move passively due to the movement of the matrix. We model this in the usual way by the term

$$\underline{J}_{\text{convection}} = n\frac{\partial \underline{\underline{u}}}{\partial t}$$

Hence the total flux is:

$$\underline{J} = -D_1\nabla n + D_2\nabla^3 n + \alpha[n\nabla(\rho + \alpha'\nabla^2\rho)] + n\frac{\partial \underline{\underline{u}}}{\partial t}$$

Mitosis. We assume cells proliferate until a limiting density N is reached, according to the logistic growth law

$$\text{mitotic rate} = rn(N-n)$$

Eqn (1) gives the conservation law for density:

$$\frac{\partial n}{\partial t} = D_1\nabla^2 n - D_2\nabla^4 n - \nabla.(\alpha n\nabla(\rho + \alpha'\nabla^2\rho)) - \nabla(n\frac{\partial \underline{\underline{u}}}{\partial t}) + rn(N-n)$$

rate of change of cell density = net flux + cell division

Mechanical Balance Equation.

We are dealing with systems in the realm of low Reynolds number (Purcell (1977)) so that the viscous and elastic forces dominate

inertial terms (i.e. motion of cells instantly ceases when the applied forces are turned off). Therefore, the restoring forces in the ECM are in equilibrium with the cell contractile forces. We model the ECM as a simple visco-elastic material with a stress tensor

$$\underline{\underline{\sigma}}_m = \underbrace{\mu_1 \frac{\partial \underline{\underline{\varepsilon}}}{\partial t} + \mu_2 \frac{\partial \theta}{\partial t} \underline{\underline{I}}}_{\text{viscous}} + \underbrace{\frac{E}{(1+\nu)} \left(\underline{\underline{\varepsilon}} + \frac{\nu}{1-2\nu} \theta \underline{\underline{I}} \right)}_{\text{elastic}} \tag{2}$$

where E is the Young's modulus, μ_1, μ_2 the shear and bulk viscosities, ν the Poisson ratio, $\theta = \nabla.\underline{u}$ the dilatation (this measures the increase in volume due to applied forces) and $\underline{\underline{I}}$ the unit tensor.

E measures the passive elastic modulus of the ECM, which we assume is initially isotropic. However, the contractile forces exerted by the cells align the collagen fibrils and thus increase the strength of the ECM. To account for this strain alignment in the simplest way (without introducing additional elastic constants), we set $E = E(\theta)$, where $E(\theta)$ is some monotonically increasing function of θ. The Poisson ratio accounts for the transverse compression of the ECM when it is stretched.

We assume the stress due to cell traction has the form

$$\underline{\underline{\sigma}}_{\text{cell-matrix}} = \tau(n) n [\rho + \beta \nabla^2 \rho] \underline{\underline{I}} \tag{3}$$

where $\tau(n) = \frac{\tau}{1+\lambda n^2}$ is the traction per cell (e.g. dyne/cm/cell). This says that as the cell density increases, the traction exerted by each cell decreases, that is, as the cells pack together their traction decreases due to contact inhibition (Trinkaus (1984)). Because the cells exert contractile forces via attachments to the ECM, traction also depends on the local matrix density $\rho(\underline{x},t)$ (short range traction) and non-local (average) matrix density $\nabla^2\rho(\underline{x},t)$ (long range traction). The parameter β measures the strength of the long range traction. Note that in an environment of large cell density and low matrix density, the cells would exert contractile forces by attaching their filopodia to other cells. Hence, we model the cell-cell contribution to active traction as

$$\underline{\underline{\sigma}}_{\text{cell-cell}} = \tau(n) [n + \beta' \nabla^2 n]. \tag{4}$$

The equation for mechanical equilibrium is

$$\nabla.\underline{\underline{\sigma}} + \rho \underline{F} = 0 \tag{5}$$

where $\underline{\underline{\sigma}} = \underline{\underline{\sigma}}_m + \underline{\underline{\sigma}}_{\text{cell-matrix}}$ and $\underline{F}$ accounts for body forces. For example, if the ECM is attached elastically to an external substratum then

$$\underline{F} = -s\underline{u}.$$

The conservation equation for matrix material has the form

$$\frac{\partial \rho}{\partial t} = \underbrace{-\nabla.(\rho \frac{\partial \underline{u}}{\partial t})}_{\text{convection}} + \underbrace{S(n,\underline{u},\rho)}_{\text{secretion}} \tag{6}$$

We shall assume in this model that secretion of matrix is negligible on the time scale of pattern formation (i.e. $S(n,\underline{u},\rho) = 0$). Equations (1), (5) and (6) constitute the field equations describing mesenchymal morphogenesis.

3. LINEAR ANALYSIS

Before linearizing, we non-dimensionalise the system. This reduces the number of parameters, making the mathematics slightly simpler. More importantly, the non-dimensional parameter groupings are biologically significant since they show which processes have equivalent effects. The non-dimensionalised system is presented in Appendix (a). The equations admit the non-trivial steady state

$$n = \rho = 1, \quad \underline{u} = \underline{0}. \tag{7}$$

Linearizing about this steady state and substituting solutions of the form $e^{\sigma(k^2)t + i\underline{k}.\underline{x}}$, where $\underline{k}$ is a wave vector, gives rise to various types of dispersion relations $\sigma(k^2)$, depending on the parameter values. (See Appendix (b) for the full dispersion relationship). We consider various $\sigma(k^2)$ behaviours and discuss the isolation of modes.

Types of $\sigma(k^2)$ behaviours. From Appendix (b) all of the dispersion relations have the form

$$\sigma(k^2) = \frac{-b(k^2) \pm \sqrt{b^2(k^2) - 4\mu k^2 c(k^2)}}{2\mu k^2} \tag{8}$$

where $b(k^2)$ and $c(k^2)$ are polynomials in k^2 and involve the parameters of the model.

The homogeneous steady state will go unstable if $R\ell(\sigma(k^2)) > 0$ for some k^2. We look for diffusion-driven instabilities wherein the homogeneous equilibrium is stable to non-spatial variations. With all parameters non-zero, it is possible to have the behaviour shown in Fig. 1(a). Since $R\ell(\sigma(k^2)) > 0 \Longleftrightarrow b(k^2) < 0$ or $c(k^2) < 0$ it may be possible (depending on the parameters satisfying certain relationships) to have the σ behaviour illustrated in Fig. 1(b).

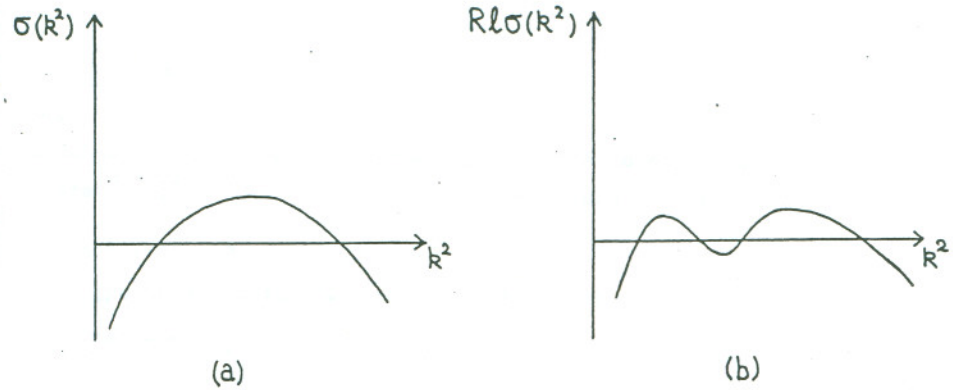

FIG. 1. Two possible dispersion behaviours. In (b), the relative values of the maxima depend on the parameter values.

We now examine the effect on the dispersion relationship of setting certain parameters equal to zero. This helps us to understand how various parameters affect the model and we can see if it is possible for simpler models to mimic the behaviour of the more complicated system.

Setting $\mu = 0$ gives $\sigma(k^2) = -c(k^2)/b(k^2)$ hence we have the possibility of infinite linear growth rates for certain non-zero modes k_i, where $b(k_i^2) = 0$. Consider, for instance, the model in which only s, r, β and τ are non-zero. In this case,

$$b(k^2) = \beta\tau k^4 + (1 - 2\tau)k^2 + s$$
$$c(k^2) = r[\beta\tau k^4 + (1 - \tau)k^2 + s] \qquad (9)$$

Fig. 2 illustrates the behaviour of $\sigma(k^2)$ as τ increases, while Fig. 3 shows the dispersion relation with $s = 0$ as well.

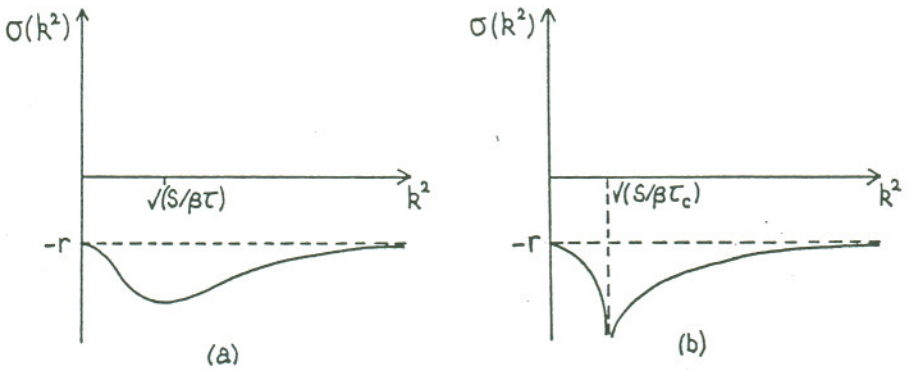

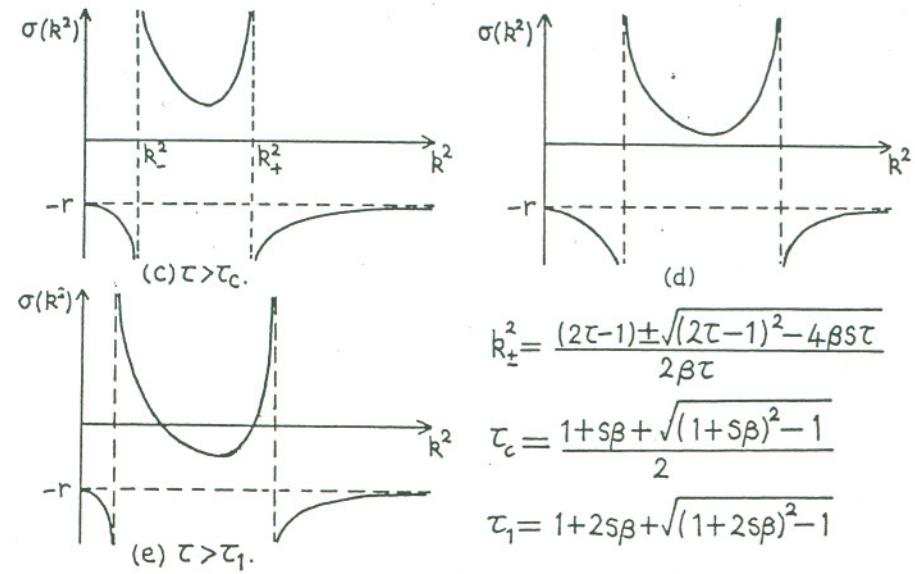

FIG. 2. Dispersion relation for the model with μ, β, r and s non-zero. Notice the character of the predicted growth rate as τ increases (a)-(e).

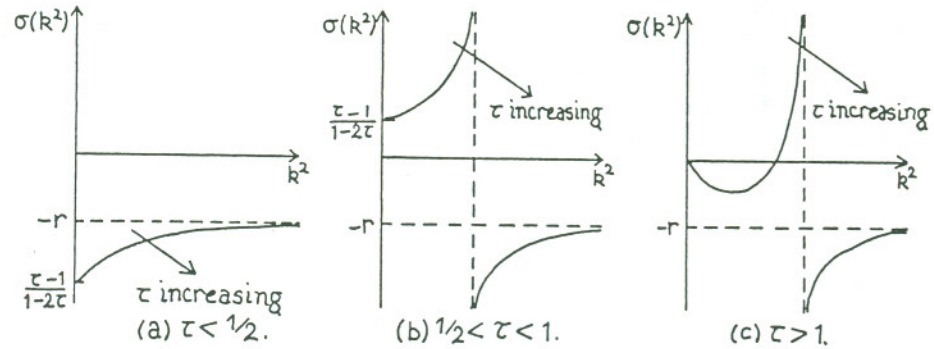

FIG. 3. Dispersion relationship in Fig. 2 with $s = 0$. As τ increases through the bifurcation value 1/2, there is a discontinuous change in $\sigma(k^2)$.

When viscosity is reintroduced the growth rate is rendered finite (Fig. 4). The central issue in the linear analysis is which of the

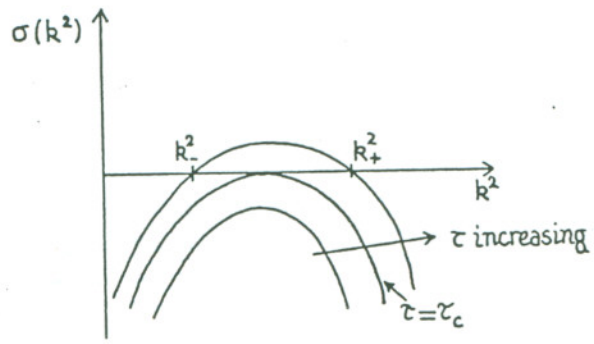

FIG. 4. Dispersion relation with μ,s,τ and β non-zero. The uniform steady state becomes unstable as τ increases.

modes $k_{\pm}$ in Fig. 2(c) grows fastest, as this is presumably the only one observed. This, together with the biological significance of such behaviour, is currently under investigation. Setting different parameters zero gives rise to a varied collection of $\sigma(k^2)$ behaviours (Murray and Oster (1984)).

Isolating modes. With fixed geometry, we show that, in order to isolate modes, it is necessary to vary at least two parameters.

Consider the one-dimensional domain [0,1] with boundary conditions $n_x = \rho_x = 0$, $u = 0$ on $x = 0,1$. The eigenfunctions are then

$$\begin{pmatrix} n \\ u \\ \rho \end{pmatrix} = \begin{pmatrix} a\cos kx \\ b\sin kx \\ c\cos kx \end{pmatrix} e^{\sigma(k^2)t} \qquad (10)$$

where $k = n\pi$ and a,b,c are arbitrary constants and the unstable modes have $R\ell\sigma(k^2) > 0$.

We can try to isolate these modes by continuously varying one parameter (that is, as the parameter changes, the first mode goes unstable by itself, then the second mode by itself, etc.). To illustrate the argument, consider the model wherein μ,s,τ and β are non-zero. (We discuss this model in more detail in section 4.) Let us increase τ while keeping the other parameters fixed. The dispersion relation is $\sigma(k^2) = -b(k^2)/\mu k^2$ where $b(k^2) = \beta\tau k^4 + (1-2\tau)k^2 + s$ and $\sigma(k^2) > 0$ if and only if $b(k^2) < 0$. The parabolas $b(k^2)$ intersect at $k^2 = 0$ and in one non-zero fixed point for

$$b(k^2,\tau_1) = b(k^2,\tau_2) \Rightarrow k^2 = 0 \text{ or } k^2 = 2/\beta.$$

Clearly one can isolate the first mode by increasing τ (Fig.5(a)). If we try to isolate mode 2, we note that the parabolas $b(k^2,\tau)$ for τ increasing must intersect at the fixed point A (see Fig.5(a)) and thus go below the parabola $b(k^2,\tau_1)$. Hence mode 1 will remain unstable and it is impossible to isolate the second mode. The difficulty is that A is fixed. For a general $b(k^2)$, it may be possible to vary the point of intersection by varying more than one parameter and thus isolate many modes (Fig.5(b)). It is clear how to generalise this simple argument for the full dispersion relationship. Note that a necessary condition for isolating modes by varying only one parameter is that it must occur quadratically in the dispersion relation.

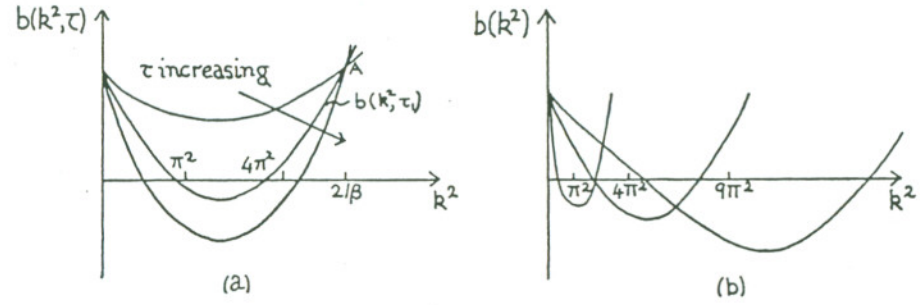

FIG.5. Isolating modes. (a) Varying τ alone will isolate one mode at most. (b) Varying two parameters for a general $b(k^2)$. (see text for detail.)

The above discussion illustrates the wide and varied behaviour that such a model may exhibit. It can be shown that the corresponding three species reaction-diffusion system can only give rise (for purely real $\sigma(k^2)$) to a dispersion relation of the form illustrated in Fig. 4. This suggests that the model here has a much richer class of pattern forming abilities than reaction-diffusion models.

4. NON-LINEAR ANALYSIS

Consider the simple model in which cell movement is by convection only and the ECM is tethered to an underlying layer (e.g. the subdermal layer in feather tract formation). The one-dimensional equations for this model are

$$\frac{\partial n}{\partial t} + \frac{\partial}{\partial x}\left(n\frac{\partial u}{\partial t}\right) = 0$$

$$\mu\frac{\partial^3 u}{\partial x^2 \partial t} + \frac{\partial^2 u}{\partial x^2} + \tau\frac{\partial}{\partial x}\left[n(\rho + \beta\frac{\partial^2 \rho}{\partial x^2})\right] - su\rho = 0 \qquad (11)$$

$$\frac{\partial \rho}{\partial t} + \frac{\partial}{\partial x}\left(\rho\frac{\partial u}{\partial t}\right) = 0$$

where we have approximated $\tau(n)$ by τn.

The dispersion relation is

$$\sigma(k^2) = 0 \text{ or } \sigma(k^2) = -\frac{(\beta\tau k^4 + (1-2\tau)k^2 + s)}{k^2} \qquad (12)$$

which is similar to that in Fig. 4: here the bifurcation

$$\tau_c = 1/2\{(1+s\beta) + [(1+s\beta)^2 - 1]^{1/2}\}$$

and we have incorporated μ into the time scale.

We perform a nonlinear bifurcation analysis similar to that in Lara and Murray (1983) as τ exceeds its critical value τ_c by setting

$$\tau = \tau_c + \varepsilon^2\delta, \quad 0 < \varepsilon << 1, \quad \delta = \pm 1 \qquad (13)$$

We look for solutions of (11) of the form

$$n(x,T,\varepsilon) = 1 + \sum_{j=1}\varepsilon^j\{A_j(\varepsilon,T)\cos jk_c x + D_j(\varepsilon,T)\sin jk_c x\}$$

$$u(x,T,\varepsilon) = \sum_{j=1}\varepsilon^j\{B_j(\varepsilon,T)\sin jk_c x + E_j(\varepsilon,T)\cos jk_c x\}$$

$$\rho(x,t,\varepsilon) = 1 + \sum_{j=1}\varepsilon^j\{C_j(\varepsilon,T)\cos jk_c x + F_j(\varepsilon,T)\sin jk_c x\} \qquad (14)$$

where $A_j(\varepsilon,T) = \sum_{i=0} A_j^i(T)\varepsilon^i$, etc. and $T = \varepsilon^2 t$.

To motivate the stretching of the time scale, consider the behaviour of $\sigma(k^2)$ for a small variation about the critical traction τ_c. A Taylor expansion of σ about k_c^2 gives

$$\sigma(k_c^2,\tau) = \sigma(k_c^2,\tau_c) + \varepsilon^2\left.\frac{\partial\sigma}{\partial\tau}\right|_{k_c^2,\tau_c} + 0(\varepsilon^4) \qquad (15)$$

($\sigma(k_c^2,\tau_c) \to 0$)

and the exponential growth term in the solution becomes $e^{0(\varepsilon^2)t}$, suggesting a slow time variable $T = \varepsilon^2 t$.

We motivate the form of solution (14) as follows. Assume

$$n = 1 + \sum_j \varepsilon^j n_j(x,t,T)$$
$$u = \sum_j \varepsilon^j u_j(x,t,T) \qquad (16)$$
$$\rho = 1 + \sum_j \varepsilon^j \rho_j(x,t,T).$$

Equating powers of ε, we have from (11)

$$\partial_t(n_1 + \partial_x u_1) = 0$$
$$\partial_{xxt}u_1 + \partial_{xx}u_1 + \tau_c\partial_x(n_1 + \rho_1) + \tau_c\beta\partial_{xxx}n_1 - su_1 = 0 \qquad (17)$$
$$\partial_t(\rho_1 + \partial_x u_1) = 0.$$

The solution of (17) is

$$\begin{pmatrix} n_1 \\ u_1 \\ \rho_1 \end{pmatrix} = \sum_j \begin{pmatrix} a_{1j}(k_j) \\ b_{1j}(k_j) \\ c_{1j}(k_j) \end{pmatrix} e^{\sigma(k_j^2)t + ik_j x} \qquad (18)$$

where $\begin{pmatrix} a_{1j}(k_j) \\ b_{1j}(k_j) \\ c_{1j}(k_j) \end{pmatrix} e^{\sigma(k_j^2)t + ik_j x}$ are the eigenfunctions of (17).

The uniform steady state becomes unstable only through the eigenfunction of wavenumber k_c, that is,

$$\sigma(k_c^2) > 0, \sigma(k_n^2) < 0 \ \forall\ k_n^2 \neq k_c^2$$

so, over a long time scale, we expect this eigenfunction to dominate. Thus the asymptotic form of (18) is (Matkowsky (1970))

$$\begin{pmatrix} n_1 \\ u_1 \\ \rho_1 \end{pmatrix} \sim \begin{pmatrix} a_{1c}(T,k_c) \\ b_{1c}(T,k_c) \\ c_{1c}(T,k_c) \end{pmatrix} e^{ik_c x} \qquad (19)$$

where the exponential term has been incorporated into the T dependence of a_{1c}, b_{1c}, c_{1c}.

Continuing this calculation at every step, the t dependence can be ignored in the subsequent analysis, and all calculations carried out asymptotically for large time. Hence we look for solutions of the form (14).

To lowest order in ε, we have

$$(A_1^0 + k_c B_1^0)_T = 0$$
$$k_c\tau_c A_1^0 + (k_c^2 + s)B_1^0 + k_c\tau_c(1 - k_c^2\beta)C_1^0 = 0 \qquad (20)$$
$$(C_1^0 + k_c B_1^0)_T = 0$$

and a similar set of equations for $\{D_1^0, E_1^0, F_1^0\}$. For the remaining calculation we shall only consider $\{A_j, B_j, C_j\}$ to simplify the analysis. (The analysis can be repeated exactly for $\{D_j, E_j, F_j\}$.)

Order ε^2 terms give

$$(A_2^0 + 2k_c B_2^0)_T + k_c A_1^0 B_{1T}^0 = 0$$
$$2k_c\tau_c A_2^0 + (4k_c^2 + s)B_2^0 + 2k_c\tau_c(1 - 4\beta k_c^2)C_2 = - k_c\tau_c(1 - k_c^2\beta)A_1^0 C_1^0 - \frac{s}{2} B_1^0 C_1^0 \qquad (21)$$
$$(C_2^0 + 2k_c B_2^0)_T + kC_1^0 B_{1T}^0 = 0$$

and order ε^3 terms give

$$-k_c^2 B_{1T}^0 - k_c\delta(A_1^0 + C_1^0) + \beta\delta k_c^3 C_1^0 + k_c\tau_c(2\beta k_c^2 - \tfrac{1}{2})A_1^0 C_2^0 + \frac{k_c\tau_c}{2}(\beta k_c^2 - 1)A_2^0 C_1^0 - \frac{s}{2}[C_1^0 B_2^0 - B_1^0 C_2^0] = 0 \qquad (22)$$

Standard nonlinear analysis simply requires successive suppression of secular terms. With the structure of our equations this is not sufficient to determine the amplitude equations. It turns out that we must use an integrated form of the conservation equations. Integrating the first and third of (20) we have three simultaneous equations for A_1^0, B_1^0 and C_1^0

$$A_1^0 + k_c B_1^0 = \gamma_1^0$$
$$k_c\tau_c A_1^0 + (k_c^2 + s)B_1^0 + k_c\tau_c(1 - k_c^2\beta)C_1^0 = 0 \qquad (23)$$
$$k_c B_1^0 + C_1^0 = \gamma_3^0$$

where γ_1^0 and γ_3^0 are constants. This system is degenerate and has non-trivial solution if and only if

$$(k_c^2(1 - \tau_c) + s)\gamma_3^0 + k_c^2\tau_c\gamma_1^0 = 0 \qquad (24)$$

i.e. there is a constraint on the initial conditions. As we have two conservation equations in the system (11) we obviously expect some constraints on initial perturbations.

Integrating the first and third of (21) gives

$$A_2^0 + 2k_c B_2^0 = A_1^{0\,2}/2 + \gamma_1^1$$
$$C_2^0 + 2k_c B_2^0 = C_1^{0\,2}/2 + \gamma_3^1 \qquad (25)$$

where γ_1^1 and γ_3^1 are constants.

Note that $\gamma_1^0 = A_1^0(0) + k_c B_1^0(0)$. If we assume initial perturbations to be $0(\varepsilon^2)$, then $\gamma_1^0 = \gamma_3^0 = 0$. Moreover, assuming initial perturbations to be $0(\varepsilon^3)$ implies $\gamma_1^1 = \gamma_3^1 = 0$. (Making these assumptions is not necessary but they help make the analysis simpler.)

We can solve the systems (23) and (25) for $B_1^0, C_1^0, A_2^0, B_2^0$ and C_2^0 in terms of A_1^0 and substituting into (22) we have the Landau equation

$$dA_1^0/dT = \delta X A_1^0 + Y A_1^{0\,3}$$

where $X = 2 - \beta k_c^2 = (2\tau_c + 1)/(2\tau_c)$ (26)

and $Y = (14\beta s\tau_c + 24\tau_c - 63\beta s - 12)/72s\beta$

Notice that the coefficient of A_1^0 is simply $\left.\frac{\partial\sigma}{\partial\tau}\right|_{k_c^2,\tau_c}$ that is, what we expect from the linear analysis.

The possible behaviours for (26) are summarised in the Table.

TABLE. Behaviour near the bifurcation when $\begin{pmatrix} n \\ u \\ \rho \end{pmatrix} = \begin{pmatrix} 1 \\ 0 \\ 1 \end{pmatrix}$,

Y as in (26).

	$Y < 0$	$Y > 0$
$\delta > 0$	A_1^0 evolves to $\sqrt{\frac{X}{\lvert Y\rvert}}$	A_1^0 goes unbounded
$\delta < 0$	A_1^0 tends to 0	there is a threshold in A_1^0 $A_1^0(0,0) < \sqrt{\frac{X}{\lvert Y\rvert}} \Rightarrow A_1^0 \to 0$ $A_1^0(0,0) > \sqrt{\frac{X}{\lvert Y\rvert}} \Rightarrow A_1^0 \to \infty$

If we are in the parameter space P (Fig. 6) the cell density evolves to the bounded steady state

$$1 + \varepsilon\sqrt{X/|Y|}\cos(k_c x) \qquad (27)$$

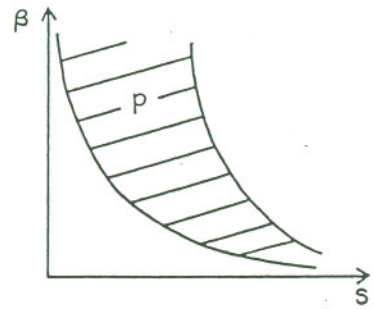

FIG. 6. Parameter space, P, in which Y > 0 and the homogeneous steady state evolves to the heterogeneous solution (27).

If we had kept in the initial constants, we would have finished up with a perturbed version of the above Landau equation, namely

$$dA_1^0/dT = C_0 + \delta(X + X_0)A_1^0 + Z_0 A_1^{0\,2} + Y A_1^{0\,3} \qquad (28)$$

where C_0, X_0 and Z_0 are functions of $\gamma_i^0, \gamma_i^1, i = 1,3$. Thus the homogeneous steady state would evolve to a heterogeneous steady state dependent on initial perturbations. Since we are dealing with small perturbations, however, these variations will also be small.

5. BIOLOGICAL APPLICATIONS

Formation of skin organs. In the early stages of skin organ development (hair, teeth, feathers, scales) dermal cells aggregate to form a regular spatial pattern. These aggregations (papillae), in association with overlapping arrays of columnar epidermal cells (placodes), lead to the formation of skin organ primordia (e.g. Rawles (1963), Wessels (1965)).

It is found that feather primordia develop in a hexagonal pattern within well-defined regions of chicken skin (pterylae). The primordia do not develop synchronously, however. In the posterior part of the spinal pteryla, for example, an initial row of feather primordia forms along the dorsal midline (Stuart and Moscona (1967), Davidson (1983)) and successive rows form on either side of this initial row.

We now apply our model to this with the following scenario: the columnar condensation forms first as dermal cells along the dorsal midline break up into isolated clumps. This could be triggered by the increasing traction of cells (or, equivalently, other parameters involved in the dimensionless traction parameter). This parameter evolution may be due, for example, to cell maturity: cells "age" into the unstable regime in parameter space wherein the homogeneous steady state becomes unstable and evolves into a heterogeneous steady state (c.f. Section 4). The tractions produced by these aggregates strain the matrix and the secondary row of papillae form at loci midway between the primary papillae, where the strain is a local minimum. This recruits other cells and thereby forms a hexagonal pattern. Fig. 7 illustrates the situation. (Numerical and analytical studies are underway to find these two-dimensional patterns).

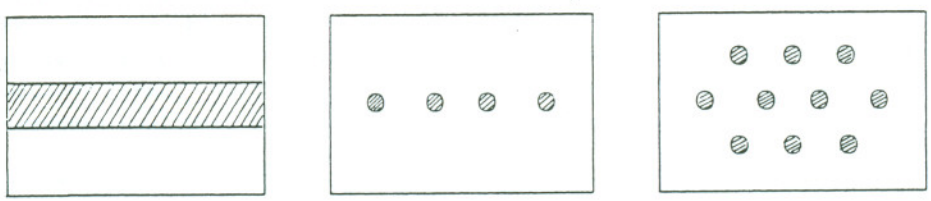

FIG. 7. Idealised section of chick pteryla. As traction increases, the uniform cell density (i) becomes unstable and forms aggregations (ii). This row of aggregates causes condensation along a neighbouring row at

interdigitating points. (iii) shows how this could give rise to hexagonal structure.

Wound healing. During wound healing, cells migrate towards the damaged site and the fibroblasts exert large contractile forces to pull the wound closed (Trinkaus (1984), Fig. 12.1). This gives rise to gross disfiguring particularly after skin graft subsequent to severe burns. The model equations are currently being studied with this application in mind. It gives rise to a formidable free boundary problem. However the potential practical rewards justify an in-depth study.

6. DISCUSSION

We have presented a model for cell aggregation, based on well documented mechanical properties of cells and extracellular matrix. We have illustrated how cell traction on an elastic substratum can produce various aggregation patterns. No directed cell migration is necessary, although if cells are motile this will merely enhance the tendency to form patterns. Thus the model illustrates how different mechanical properties of the cells can lead to cell pattern. The predictions of the model can be (and are being) tested experimentally as, in principle, all the parameters are measurable.

Mechanical models can thus lead to a greater understanding, biologically, of the phenomenon of development. For the mathematician and numerical analyst, the models provide an interesting and formidable class of problems to be investigated.

Acknowledgements: PKM wishes to thank the Department of Education of Northern Ireland for a postgraduate studentship. GFO would like to acknowledge support from the Science and Engineering Research Council of Great Britain (Grant GR/C/63595) for a visit to the Centre for Mathematical Biology in Oxford.

APPENDIX

(a) Let L, T_0 be typical length and time scales respectively and let ρ_0 be a typical matrix density. With the following dimensionless quantities

$$\tilde{n} = n/N,\ \tilde{\rho} = \rho/\rho_0,\ \tilde{\underline{u}} = \frac{\underline{u}}{L},\ \tilde{t} = t/T_0,\ \tilde{\underline{x}} = \underline{x}/L,\ \tilde{D}_1 = D_1T_0/L^2,\ \tilde{\lambda} = \lambda N^2,$$

$$\tilde{\beta} = \beta/L^2,\ \tilde{s} = s\rho_0L^2(1+\nu)/E,\ \tilde{D}_2 = D_2T_0/L^4,\ \tilde{\alpha} = \alpha\rho_0T_0/L^2,\ \tilde{\alpha}' = \alpha'/L,$$

$$\tilde{r} = rNT_0,\ \tilde{\mu}_1 = \mu(1+\nu)/T_0E,\ \tilde{\mu}_2 = \mu_2(1+\nu)/T_0E,\ \tilde{\tau} = \tau N\rho_0(1+\nu)/E$$

the system (1), (5), (6) becomes (dropping tildes)

$$\frac{\partial n}{\partial t} = D_1\nabla^2 n - D_2\nabla^4 n - \alpha\nabla.[n\nabla(\rho+\alpha'\nabla^2\rho)] - \nabla.[n\frac{\partial \underline{\underline{u}}}{\partial t}] + rn(1-n)$$

$$\nabla.[\mu_1\frac{\partial \underline{\underline{\varepsilon}}}{\partial t} + \mu_2\frac{\partial \theta}{\partial t}\underline{\underline{I}} + (\underline{\underline{\varepsilon}} + \hat{\nu}\theta\underline{\underline{I}}) + \frac{\tau n}{1+\lambda n^2}\{\rho + \beta\nabla^2\rho\}\underline{\underline{I}}] = s\underline{u}\rho$$

$$\frac{\partial \rho}{\partial t} + \nabla.(\rho\frac{\partial \underline{u}}{\partial t}) = 0$$

where $\hat{\nu} = \frac{\nu}{1-2\nu}$.

Notice that by taking different values for T_0, we can work on different time scales, e.g. we could work on the haptotactic time scale by setting $T_0 = L^2/\alpha\rho_0$ (Oster, Murray and Harris (1983)).

(b) Linearizing about the steady state $n = \rho = 1$, $u = 0$ by setting $n = 1 + \tilde{n}$, $\rho = 1 + \tilde{\rho}$, $u = \tilde{u}$ (where the tilde variables are small variations from the steady state), we find the dispersion relation, in the usual way, by looking for solutions

$$\begin{pmatrix} \tilde{n} \\ \tilde{u} \\ \tilde{\rho} \end{pmatrix} \propto e^{\sigma(k^2)t + i\underline{k}.\underline{x}}$$

In one dimension, this gives rise to the relationship

$$\sigma(k^2)(\mu k^2\sigma^2(k^2) + b(k^2)\sigma(k^2) + c(k^2)) = 0$$

where

$$b(k^2) = \mu D_2k^6 + (\tau\beta/(1+\lambda) + \mu D_1)k^4 + (1+\mu r - 2\tau/(1+\lambda)^2)k^2 + s,$$

$$c(k^2) = \tau/(1+\lambda)\beta D_2k^8 + (\tau/(1+\lambda)\ (\beta D_1 - D_2 + \alpha\alpha'(1-2\lambda/(1+\lambda)) + D_2)k^6$$

$$+[\tau/(1+\lambda)(r\beta - D_1 - \alpha(1-2\lambda/(1+\lambda)) + sD_2 + D_1]k^4 + (sD_1+r-r\tau/(1+\lambda))k^2$$

$$+ rs$$

where $\mu = \mu_1 + \mu_2$, and we have normalised μ, τ and s by dividing by $(1+\hat{\nu})$.

References

Davidson, D. (1983). The mechanism of feather pattern development in the chick. 1. The time determination of feather position. J.Embryol. Exp. Morph., 74, 245-259.

Gierer, A. & Meinhardt, H. (1972). A theory of biological pattern formation. Kybernetik, 12, 30-39.

Harris, A.K. (1973) Behaviour of cultured cells on substrata of variable adhesiveness. Exp. Cell Res., 77, 285-297.

Harris, A.K., Stopak, D. & Wild, P. (1981). Fibroblast traction as a mechanism for collagen morphogenesis. Nature, 290, 249-251.

Lara Ochoa, F. & Murray, J.D. (1983). A non-linear analysis for spatial structure in a reaction diffusion model. Bull.Math.Biol. 45, 917-930.

Matkowsky, B.J. (1970). A simple non-linear dynamic stability problem. Bull. Amer. Math. Soc., 76, 620-625.

Meinhardt, H. (1982). Models of biological pattern formation. Academic Press, London.

Murray, J.D. (1977). Lectures on non-linear differential equation models in biology. Oxford University Press: Oxford.

Murray, J.D. (1981). On pattern formation mechanisms for Lepidopteran wing patterns and mammalian coat markings. Phil. Trans. Roy. Soc. Lond. B295, 473-496.

Murray, J.D. & Oster, G.F. (1984). Generation of biological pattern and form. I.M.A. J. Maths. Appl. to Biol. & Med., 1,

Oster, G.F., Murray J.D. & Harris, A.K. (1983). Mechanical aspects of mesenchymal morphogenesis. J. Embryol. Exp. Morph. 78, 83-125.

Purcell, E.M. (1977). Life at low Reynolds number. Amer. J. of Phys., 45, 3-11.

Rawles, M. (1963). Tissue interactions in scale and feather development as studied in dermal-epidermal recombinations. J. Embryol. Exp. Morph., 11, 765-789.

Saunders, J.W. & Gasseling, M.T. (1968). Ectodermal-mesenchymal interactions in the origin of limb symmetry. In epithelial-mesenchymal interactions (ed. R. Fleischmajer & R.E. Billingham), pp.78-97.

Smith, J.C., Tickle, C. & Wolpert, L. (1978). Attenuation of positional signalling in the chick limb by high doses of γ-radiation. Nature, 272, 612-613.

Smith, J.C. & Wolpert, L. (1981). Pattern formation along the antero-posterior axis of the chick wing: the increase in width following a

polarizing region graft and the effect of X-irradiation. J. Embryol. Exp. Morph., 63, 127-144.

Stuart, E.S. & Moscona, A.A. (1967). Embryonic morphogenesis: Role of fibrous lattice in the development of feathers and feather patterns. Science, 157, 947-948.

Thomas, D. (1975). In analysis and control of immobilized enzyme systems, (Thomas, D. & Kernevez, J.P. eds.) New York: Springer-Verlag, pp. 115-150.

Tickle, C. (1981). The number of polarizing region cells required to specify additional digits in the developing chick wing. Nature, 289, 295-298.

Trinkaus, J.P. (1984). Cells into organs: The forces that shape the embryo. (Prentice-Hall).

Turing, M.A. (1952). The chemical basis of morphogenesis. Phil. Trans. Roy. Soc. Lond., B237, 37-73.

Wessells, N.K. (1965). Morphology and proliferation during early feather development. Dev. Biol., 12, 131-153.

Wolpert, L. (1969). Positional information and the spatial pattern of cellular differentiation. J. Theor. Biol., 25, 1-47.

Wolpert, L. & Hornbruch, A. (1981). Positional signalling along the anteroposterior axis of the chick wing. The effect of multiple polarizing region grafts. J. Embryo. Exp. Morph., 63, 145-159.